Journal of Visualized Experiments

Cerebral Blood Flow-Based Resting-State Functional Connectivity of the Human Brain Measured by Optical Diffuse Correlation Spectroscopy

--Manuscript Draft--

Article Type:	Invited Methods Article - JoVE Produced Video
Manuscript Number:	JoVE60765R2
Full Title:	Cerebral Blood Flow-Based Resting-State Functional Connectivity of the Human Brain Measured by Optical Diffuse Correlation Spectroscopy
Section/Category:	JoVE Bioengineering
Keywords:	diffuse correlation spectroscopy; blood flow; functional connectivity; cerebral hemodynamics; medicine; Neuroscience; Biomedical Engineering; physiology.
Corresponding Author:	Ulas Sunar, Ph.D. Wright State University Dayton, OH UNITED STATES
Corresponding Author's Institution:	Wright State University
Corresponding Author E-Mail:	ulas.sunar@wright.edu
Order of Authors:	Chien Poon
	Ben Rinehart
	Jun Li
	Ulas Sunar, Ph.D.
Additional Information:	
Question	**Response**
Please indicate whether this article will be Standard Access or Open Access.	Standard Access (US$2,400)
Please indicate the **city, state/province, and country** where this article will be **filmed**. Please do not use abbreviations.	Dayton, OH

TITLE:

Cerebral Blood Flow-Based Resting State Functional Connectivity of the Human Brain Using Optical Diffuse Correlation Spectroscopy

AUTHORS AND AFFILIATIONS:

Chien Poon[1], Ben Rinehart[1], Jun Li[1,2], Ulas Sunar[1]

[1]Department of Biomedical, Industrial and Human Factors Engineering, Wright State University, Fairborn, OH, USA

[2]South China Academy of Advanced Optoelectronics, South China Normal University, Guangzhou, China

Corresponding Author:

Ulas Sunar (ulas.sunar@wright.edu)

Email Addresses of Co-Authors:

Chien Poon (poon.4@wright.edu)

Ben Rinehart (rinehart.32@wright.edu)

Jun Li (jun.li@coer-scnu.org)

KEYWORDS:

diffuse correlation spectroscopy, blood flow, functional connectivity, cerebral hemodynamics medicine, neuroscience, biomedical engineering, physiology

SUMMARY:

This protocol demonstrates how to measure resting state functional connectivity in the human prefrontal cortex using a custom-made diffuse correlation spectroscopy instrument. The report also discuss practical aspects of the experiment as well as detailed steps for analyzing the data.

ABSTRACT:

To obtain a comprehensive understanding of the human brain, utilization of cerebral blood flow (CBF) as a source of contrast is desired because it is a key hemodynamic parameter related to cerebral oxygen supply. Resting state low frequency fluctuations based on oxygenation contrast have been shown to provide correlations between functionally connected regions. The presented protocol uses optical diffuse correlation spectroscopy (DCS) to assess blood flow-based resting state functional connectivity (RSFC) in the human brain. Results of CBF-based RSFC in human frontal cortex indicate that intra-regional RSFC is significantly higher in the left and right cortices compared to inter-regional RSFC in both cortices. This protocol should be of interest to researchers who employ multi-modal imaging techniques to study human brain function, especially in the pediatric population.

INTRODUCTION:

When the brain is in a resting state, it demonstrates a high synchronization of spontaneous

activity in functionally related regions, which can be located close in proximity or from a distance. These in-sync regions are known as functional networks[1–9]. This phenomenon was first uncovered by a functional magnetic resonance imaging (fMRI) study using blood oxygen level-dependent (BOLD) signals that indicate oxygenation levels of the cerebral blood[5,10], also known as resting state functional connectivity (RSFC). Abnormalities in RSFC have been associated with brain disorders such as autism[11], Alzheimer's[12], and depression[13]. Thus, RSFC is a valuable tool for studying patients with disorders who have trouble performaning task-based assessments. However, many patients, such as young autistic children, are poor candidates for assessment by fMRI, as it requires remaining still inside of a confined space for extended periods of time[14,15]. Optical imaging is fast and wearable; thus, it is suitable for a majority of patients, particularly the pediatric population[16–24]. Utilizing these advantages, functional near-infrared spectroscopy (fNIRS), which can quantify hemoglobin concentration and oxygen saturation parameters in the brain, is used to measure RSFC in humans (including the pediatric population[4,8,25] and patients with autism[11]).

Optical diffuse correlation spectroscopy (DCS), a relatively new optical technique, can quantify cerebral blood flow, which is an important parameter that associates oxygen supply with metabolism[6,17,26–29]. Optical flow contrast quantified by DCS has been shown to have higher sensitivity in the brain compared to oxygenation contrast[30]. Thus, utilizing DCS-derived CBF parameters for assessing RSFC is advantageous.

DCS is sensitive to moving blood cells. When diffusing photons scatter from moving blood cells, this causes the intensity of detected light to fluctuate over time. DCS measures a time-based intensity autocorrelation function and its decay rate are dependent on the optical parameters and blood flow. These values are ultimately used to obtain the cerebral blood flow index (CBFi). With faster moving blood cells, the intensity autocorrelation function decays faster. Therefore, information about motion deep beneath the tissue surface can be derived (e.g., in the brain) from measurements of diffusing light fluctuations over time[27,31–35]. DCS is a technique complementary to the widely known fNIRS that measures blood oxygenation[17,36]. Since both fNIRS and DCS are optical brain imaging techniques with high temporal resolution in the range of milliseconds, the optical imaging set-ups are far less sensitive to motion artifacts than fMRI. They have also been successfully used for functional brain imaging in pediatric populations, including very young infants[16]. Previously, superficial blood flow measurements have been used to assess RSFC in preclinical studies in mice[37]. Here, blood flow parameters are used to quantify RSFC in nine healthy adults as a proof-of-concept study[38,39].

In this study, a commercial FD-fNIRS system and custom DCS system is used (**see Table of Materials**). The DCS that was built in-house is comprised of two 785 nm, 100 mW, long coherence length continuous-wave lasers that are coupled to an FC connector and eight single-photon counting machines (SPCM) connected to an auto-correlator. A custom software graphical user interface (GUI) was also made specifically for this system to display and save the photon counts, autocorrelation curves, and semi-quantitative blood flow of each SPCM channel in real-time. The parts in this system are commonly used for DCS[16,17,31,32,40–44], and the results obtained have also been verified in-house and used in a recent study[39].

PROTOCOL:

The protocol was approved by the Institutional Review Board at Wright State University, and informed consent was obtained from each participant prior to the experiment.

1. Subject preparation

1.1) Power up the FD-fNIRS and DCS system to warm up for at least 10 min (see sections 2 and 3 for more details) before starting any measurements of the subject. An example of subject measurement with the compact DCS instrument is shown in **Figure 1**.

1.2) First, use a tape measure to measure the distance between the nasion to inion on each subject's head (**Figure 2A**).

1.3) With the nasion as the starting point, mark the location that is 10% of the distance to the inion with an ink marker. This denotes the point between Fp1 and Fp2 of the EEG 10/20 montage (**Figure 2A**).

1.4) Using an EEG 10/20 cap (see **Table of Materials**), adjust the cap so that the marked point is between Fp1 and Fp2.

1.5) Mark the point between Fp1 and F7 (left cortex) and the point between Fp2 and F8 (right cortex). This represents the boundaries between the superior prefrontal cortex and dorsolateral prefrontal cortex (DLFC) and between the DLFC and inferior prefrontal cortex (IFC), respectively, for the left and right hemispheres (**Figure 2A**).

1.6) Using a 3D-printed probe, place the multi-mode fibers (MMF) on the newly marked points (points "S" on **Figure 2C**) and connect each to the 785 nm laser light source (**Figure 2B,C**).

1.7) Place the single-mode fibers (SMFs) 2.75 cm away from the MMF. Two fibers should be placed on the DLFC (locations "DLFC,1" and "DLFC,2") and one on the IFC (location "IFC"). The placement of the SMF is replicated on each side of the cortex for a total of six SMFs (**Figure 2c**).

1.8) Place another SMF 1 cm below the MMF at location "D_S" in both sides of the cortex (for the detection of blood flow in the scalp) and connect each of the SMFs to individual single-photon counting machines (**Figure 2C**).

2. FD-fNIRS settings and calibration

2.1) Turn off any lights and turn on the FD-fNIRS system to prepare for calibration.

CAUTION: As a general precaution, do not look directly at the light sources and fiber outputs, as this may cause eye damage. Use an IR sensor card (**Table of Materials**).

2.2) Avoid unnecessary exposure of the detectors to room light levels to maintain noise-free operation and avoid damage to the detectors.

2.3) Warm the light sources and detectors by powering up the system and letting it run for at least 10 min (preferably, 20 min minimum and 1 h maximum for optimal accuracy and stability) with the light on, modulation on, and detector voltage on.

2.4) Run GUI-based data acquisition software. Adjust the detector gain to achieve an optimal signal with the sensor attached and secured to a calibration phantom (polydimethylsiloxane-based phantom of known optical properties, see **Table of Materials**) by pressing the "auto-bias" button. If the overvoltage warning flashes, lower the gain.

2.5) After adjusting the detector gain to get the maximum signal, disconnect one of the source fibers from the detector and verify that the direct current (DC) is less than 20 counts per measurement period for the corresponding source fiber. If it is greater than this value, there may be excessive room light leaking into the detector[45]. If this is the case, the system should be powered down, then any excess light in the room should be blocked/removed and steps 2.4–2.5 repeated.

2.6) Verify the proper signal level from every source and detector. The system defines this as above 100 and below 1,500 counts per measurement cycle.

2.7) Perform calibration by pressing the "Calibrate" button in the GUI. The system will take measurements and apply calibration factors to correctly measure the optical properties of the known phantom. These calibration factors are saved and applied automatically to the in vivo measurements.

2.8) Log the calibration data, which will provide a record of system performance on a standard phantom.

3. DCS settings

CAUTION: As a general precaution, do not look at the light sources and fiber outputs directly to avoid potential eye damage. Use the IR sensor card (see **Table of Materials**).

3.1) Avoid unnecessary exposure of the detectors (i.e., room light) to obtain accurate raw data for the autocorrelation curves and prevent damage to the detectors.

3.2) Warm up the DCS laser light sources and SPCM (see **Table of Materials**) by switching them to the "on" position and allowing them to run for at least 10 min (preferably, 20 min minimum and 1 h maximum for optimal accuracy and stability).

3.3) Run GUI-based DCS data acquisition software, which displays the photon counts for each detector and semi-quantitative real-time blood flow values. Adjust the fiber position,

angle (fiber face should be perpendicular to the skin surface), and data acquisition timing to obtain a signal of at least 5,000 counts/s (for an adequate signal to noise ratio) and below 1,000,000 counts/s (to avoid damaging detectors) **(Figure 3A)**.

3.4) Verify sufficient photon count levels (from step 3.3) from each detector by checking the photon count level and near real-time autocorrelation curves shown on the monitor.

3.5) Verify sufficient fiber contact without any ambient light leakage by checking the y-intercept of the autocorrelation curve displayed on the monitor. The optimal value is ~1.5 without the use of polarizers **(Figure 3B)**.

3.6) Verify that the probe and measurements are not prone to motion artifacts by tightening the elastic band so that it is tight enough to resist motion but loose enough to prevent any discomfort to the subject. The user should also check the autocorrelation curves on the monitor concurrently such that the autocorrelation curve decays to 1 for longer correlation time ($\tau > 10$ ms) **(Figure 3C)**.

4. Data collection

4.1) Instruct the subject to minimize any movements during the 8 min measurement.

4.2) Turn off the lights and make sure that the subject is seated in a comfortable position with his/her eyes closed.

4.3) Perform a baseline FD-fNIRS measurements using by placing the FD-fNIRS system optical probe on the forehead adjacent to the DCS probe. Then, press the "Acquire" button in the FD-fNIRS acquisition GUI. This data will provide static optical properties, absorption parameters, and scattering parameters (μ_a, μ_s') that will be used for quantification of the dynamic optical parameter, CBFi[17,20].

4.4) After completion of the FD-fNIRS measurements, begin data acquisition on the optical DCS measurements by pressing the "Run" button in the DCS data acquisition GUI. Collect data for a total of 8 min with a maximum 2 s integration time (less is preferred, depending on the signal-to-noise ratio for each subject).

4.5) If necessary, repeat the experiment within 1 h of the initial experiment or repeat the experiment during a similar time of day to reduce external variations such as fatigue, stimulants, or temperature.

5. Data analysis

5.1) For FD-fNIRS data, extract the optical absorption and scattering properties (μ_a, μ_s') that are processed by the slope method[46–53].

5.2) For DCS, since post-processing is needed, import the auto-correlation raw data from each of the eight channels into the data analysis software.

5.3) CBF-related parameter quantification is detailed in recent reviews[6,27,54]. Briefly, from the normalized intensity autocorrelation function (g_2 [r,τ]), extract the normalized diffuse electric field temporal autocorrelation function (g_1 [r,τ]) using the Siegert relation: g_2 (r,τ) = 1 + β|g_1 (r,τ)|^2.

NOTE: β is a constant, proportional to the number of spatial modes detected[6,17,27,55,56], ranges from 0 to 1, and obtained by fitting the (normalized) electric field autocorrelation function g_1.

5.4) To obtain a blood flow-related parameter (αD_B) from the fit, use the analytical solution for g_1[6,27,54] and fit the data to the model or decay rate:

$$k^2(\tau) = 3\mu_a\mu_s^{'} + \mu_s^{'\,2}k_o^2\alpha(6D_B\tau).$$

NOTE: In the equation above, k_o is the wavenumber of light in the medium, α is a factor proportionate to tissue blood volume fraction, and D_B is the effective Brownian coefficient. αD_B can be defined as the blood flow index (BFI)[6,54] or CBFi[17]. Here, CBFi is used.

5.5) Fit the model using the optical parameters obtained from FD-fNIRS. The main parameters to fit for are CBFi and β.

NOTE: **Figure 3A** shows representative data that is sufficient for analysis. DCS data is discarded if (1) the autocorrelation function is significantly lower than 1.5 (β < 0.5) (i.e., in the case of **Figure 3B,** where the function is ~1.2, β < 0.2, due to room light leakage) or if (2) the autocorrelation curve does not decay to 1 for longer correlation time (τ > 10 ms) (i.e., in the case of **Figure 3C**, where the motion artifact, such head or probe movement, leads to unusable data).

5.6) Detrend the quantified results using a second-order polynomial fit to remove slow drift (**Figure 4A**).

5.7) Use a zero-phase second-order Butterworth filter with a passband of 0.009–0.080 Hz to remove any unwanted brain frequencies such as Mayer waves (**Figure 4A**).

5.8) Use linear regression to obtain the residuals from each channel against the short distance measurement to remove the superficial scalp signals on each side of the cortex (**Figure 4B**).

5.9) Calculate the Pearson's correlation coefficient between each pair of channels to identify the resting state functional connectivity between brain regions (**Figure 5**).

5.10) Transform the correlation value into a z-value using a Fisher Z transformation and perform a *t*-test to obtain the p-value (**Figure 5**). Use false discovery rate (FDR) for multiple comparisons correction.

REPRESENTATIVE RESULTS:

The feasibility of using DCS to measure functional connectivity was successfully demostrated[39]. The resting state functional connectivity in the prefrontal cortices of nine subjects was measured. The results (mean ± SD) indicated a higher correlation in the intra-regional region of the left (0.64 ± 0.25) and right (0.62 ± 0.23) cortices, compared to the inter-regional region of the left (0.32 ± 0.32), (0.34 ± 0.27) and right (0.34 ± 0.29), (0.34 ± 0.26) cortices. **(Figure 5)**. Power analysis with a power of 0.8 and significance level of 0.05 was also performed, which resulted in a power of 0.82 with sample size of eight (below the number of subjects analyzed in this study).

To test if there was a significant difference between inter-regional RSFC and intra-regional RSFC, the correlation value was transformed into a z-value using a Fisher Z transformation, then a t-test was performed to compare inter- and intra-regional RSFC of both cortices. This resulted in p-values of ≤0.0002, signifying a significant difference that has been demonstrated in previous fNIRS studies[8,25] **(Figure 5)**. To determine if there was any difference between symmetrical brain regions (left and right cortices), a t-test was performed. This resulted in p-values of >0.8, signifying that there was no significant difference between similar brain regions on either side of the cortex.

FIGURE AND TABLE LEGENDS:

Figure 1: Experimental set-up.

Figure 2: Probe schematic and placement. (A) Placement of the probes as shown on the EEG 80-20 system map. **(B)** An example of the 3D-printed probe with optical fibers worn by the subject. **(C)** The CAD model of the location of the detectors (D) and sources (S) in the dorsolateral frontal cortex (DLFC) and inferior frontal cortex (IFC).

Figure 3: Representative sample of data using detectors in the same region at the same source-detector separation. Shown is an autocorrelation curve (g2) with respect to the lag time (τ). (**A**) Data when the probe has sufficient contact, showing high counts and a good fit to the analytical model. (**B**) Data (exaggerated) with ambient light leaking into the probe as observed by a lower y-intercept (beta). This is usually due to a combination of poor contact and strong background light, requiring adjustments to be made. (**C**) Data (exaggerated) with a motion artifact while the g2 curve is being averaged.

Figure 4: Analysis of representative data obtained from one subject. (A) A plot of the power spectrum after each of the processing steps. **(B)** An example showing the time series of the normalized blood flow signal on one of the channels before and after regression of the short distance channel (scalp signal).

Figure 5: Resting state functional connectivity in prefrontal cortices of all subjects. Group average for inter-regional region ($DLFC_1$-IFC and $DLFC_2$-IFC) of the left cortex (0.32 ± 0.32), (0.34 ± 0.27) and right cortex (0.34 ± 0.29), (0.34 ± 0.26). Group average for intra-regional region of the left cortex (0.64 ± 0.25) and right cortex (0.62 ± 0.23). Error bar indicates SD across all subjects. The t-test shows the difference between intra- and inter-regional RSFC of both cortices is significant with $p \leq 0.0002$, while there was no significant difference between the left and right cortex (t-test = $p > 0.8$). False discovery rate (FDR) was used for multiple comparisons correction.

DISCUSSION:

To determine whether CBF as measured by DCS accurately detected RSFC, two areas of the brain with known RSFC properties were examined. Functional connectivity between DLFC regions and between DLFC and IFC is assumed to exist[57–59]. Connectivity between two sites within the left and right DLFC was chosen, because the intra-regional connectivity is usually higher. Also, connectivity between the IFC and the DLFC was chosen, as the inter-regional connectivity is known to be weaker.

The DCS technique showed high connectivity within the DLFC areas but lower connectivity between the IFC and DLFC areas, which is consistent with similar studies performed with other methods such as fMRI. These results demonstrate the potential of DCS as a non-invasive means to assess RSFC in humans. When combined with other imaging modalities such as fNIRS, accurate characterization of neuronal diseases such as autism becomes viable. Although concurrent measurements of fNIRS and DCS remain a challenge, several approaches to this problem have been explored[19-21,23,27,28,60–65]. In a pilot study, the isolated, lighter DCS probes were chosen for better contact. In the future, the probe design can be improved, fNIRS fibers can be inserted next to DCS fibers, and light sources can be sequentially illuminated as previously demonstrated. In summary, DCS will serve as a complement to other techniques and become a useful tool for non-invasive assessment of brain function in young and disabled patients.

ACKNOWLEDGMENTS:

The authors would like to acknowledge financial support from the Ohio Third Frontier to the Ohio Imaging Research and Innovation Network (OIRAIN, 667750), and the National Natural Science Foundation of China (No. 81771876).

DISCLOSURES:

The authors declare no competing financial interests.

REFERENCES:

1. Cohen, A. L. et al. Defining functional areas in individual human brains using resting functional connectivity MRI. *NeuroImage*. **41** (1), 45–57 (2008).
2. Pizoli, C. E. et al. Resting state activity in development and maintenance of normal brain

function. *Proceedings of the National Academy of Sciences of the United States of America*. **108** (28), 11638–11643 (2011).
3. Duan, L., Zhang, Y. J., Zhu, C. Z. Quantitative comparison of resting state functional connectivity derived from fNIRS and fMRI: A simultaneous recording study. *NeuroImage*. **60** (4), 2008–2018 (2012).
4. White, B. R. et al. Resting state functional connectivity in the human brain revealed with diffuse optical tomography. *NeuroImage*. **47** (1), 148–156 (2009).
5. Biswal, B., Yetkin, F. Z., Haughton, V. M., Hyde, J. S. Functional connectivity in the motor cortex of resting human brain using echo-planar MRI. *Magnetic resonance in medicine : official journal of the Society of Magnetic Resonance in Medicine/Society of Magnetic Resonance in Medicine*. **34** (4), 537–41 (1995).
6. Mesquita, R. C. et al. Direct measurement of tissue blood flow and metabolism with diffuse optics. *Philosophical Transactions of the Royal Society A: Mathematical, Physical and Engineering Sciences*. doi: 10.1098/rsta.2011.0232 (2011).
7. Zhang, H. et al. Test–retest assessment of independent component analysis-derived resting state functional connectivity based on functional near-infrared spectroscopy. *NeuroImage*. **55** (2), 607–615 (2011).
8. Lu, C. M. et al. Use of fNIRS to assess resting state functional connectivity. *Journal of Neuroscience Methods*. **186** (2), 242–249 (2010).
9. Zhang, Y. -J. et al. Detecting Resting state Functional Connectivity in the Language System using Functional Near-Infrared Spectroscopy. *Journal of Biomedical Optics*. **15** (4), 047003 (2010).
10. Fransson, P. Spontaneous low-frequency BOLD signal fluctuations: An fMRI investigation of the resting state default mode of brain function hypothesis. *Human Brain Mapping*. doi: 10.1002/hbm.20113 (2005).
11. Li, J. et al. Characterization of autism spectrum disorder with spontaneous hemodynamic activity. *Biomedical Optics Express*. doi: 10.1364/boe.7.003871 (2016).
12. Sheline, Y. I., Raichle, M. E. Resting state functional connectivity in preclinical Alzheimer's disease. *Biological Psychiatry*. doi: 10.1016/j.biopsych.2012.11.028 (2013).
13. Mulders, P.C ., van Eijndhoven, P. F., Schene, A. H., Beckmann, C. F., Tendolkar, I. Resting state functional connectivity in major depressive disorder: A review. *Neuroscience and Biobehavioral Reviews*. doi: 10.1016/j.neubiorev.2015.07.014 (2015).
14. Kiviniemi, V. et al. Slow vasomotor fluctuation in fMRI of anesthetized child brain. *Magnetic Resonance in Medicine*. doi: 10.1002/1522-2594(200009)44:3<373::AID-MRM5>3.0.CO;2-P (2000).
15. Fransson, P. et al. Resting state networks in the infant brain. *Proceedings of the National Academy of Sciences of the United States of America*. doi: 10.1073/pnas.0704380104 (2007).
16. Durduran, T., Yodh, A. G. Diffuse correlation spectroscopy for non-invasive, micro-vascular cerebral blood flow measurement. *Neuroimage*. **85**, 51–63 (2014).
17. Buckley, E. M., Parthasarathy, A. B., Grant, P. E., Yodh, A. G., Franceschini, M. A. Diffuse correlation spectroscopy for measurement of cerebral blood flow: future prospects. *Neurophotonics*. **1** (1), 011009 (2014).
18. Buckley, E. M. et al. Cerebral hemodynamics in preterm infants during positional

intervention measured with diffuse correlation spectroscopy and transcranial Doppler ultrasound. *Optics Express*. doi: 10.1364/oe.17.012571 (2009).
19. Dehaes, M. et al. Cerebral oxygen metabolism in neonatal hypoxic ischemic encephalopathy during and after therapeutic hypothermia. *Journal of Cerebral Blood Flow and Metabolism*. doi: 10.1038/jcbfm.2013.165 (2014).
20. Lin, P. Y. et al. Non-invasive optical measurement of cerebral metabolism and hemodynamics in infants. *Journal of Visualized Experiments.* (2013).
21. Lin, P.Y. et al. Regional and hemispheric asymmetries of cerebral hemodynamic and oxygen metabolism in newborns. *Cerebral Cortex*. **23** (2), doi: 10.1093/cercor/bhs023 (2013).
22. Busch, D. R. et al. Cerebral Blood Flow Response to Hypercapnia in Children with Obstructive Sleep Apnea Syndrome. *Sleep*. doi: 10.5665/sleep.5350 (2016).
23. T., D. et al. Cerebral oxygen metabolism (CMRO2) reactivity to hypercapnia in neonates with severe congenital heart defects measured with diffuse optics. *Journal of Cerebral Blood Flow and Metabolism*. doi: http://dx.doi.org/10.1038/jcbfm.2009.132 (2009).
24. Durduran, T. et al. Optical measurement of cerebral hemodynamics and oxygen metabolism in neonates with congenital heart defects. *Journal of Biomedical Optics*. doi: 10.1117/1.3425884 (2010).
25. Mesquita, R. C., Franceschini, M. A., Boas, D. A. Resting state functional connectivity of the whole head with near-infrared spectroscopy. *Biomedical optics express*. **1** (1), 324–336 (2010).
26. Boas, D. A., Franceschini, M. A. Haemoglobin oxygen saturation as a biomarker: The problem and a solution. *Philosophical Transactions of the Royal Society A: Mathematical, Physical and Engineering Sciences*. doi: 10.1098/rsta.2011.0250 (2011).
27. Durduran, T., Yodh, A. G. Diffuse correlation spectroscopy for non-invasive, micro-vascular cerebral blood flow measurement. *NeuroImage*. doi: 10.1016/j.neuroimage.2013.06.017 (2014).
28. Yu, G. Diffuse Correlation Spectroscopy (DCS): A Diagnostic Tool for Assessing Tissue Blood Flow in Vascular-Related Diseases and Therapies. *Current Medical Imaging Reviews*. **8**, 194–210 (2012).
29. Yu, G., Durduran, T., Zhou, C., Cheng, R., Yodh, A. G. Near-Infrared Diffuse Correlation Spectroscopy for Assessment of Tissue Blood Flow. *Handbook of Biomedical Optics*. 195–216 (2011).
30. Selb, J. et al. Sensitivity of near-infrared spectroscopy and diffuse correlation spectroscopy to brain hemodynamics: simulations and experimental findings during hypercapnia. *Neurophotonics*. **1** (1), (2014).
31. Cheung, C. et al. In vivo cerebrovascular measurement combining diffuse near-infrared absorption and correlation spectroscopies. *Physics in Medicine and Biology*. **46** (8), 2053–2065 (2001).
32. Mesquita, R. C. et al. Direct measurement of tissue blood flow and metabolism with diffuse optics. *Philos Trans A Math Phys Eng Sci*. **369** (1955), 4390–4406 (2011).
33. Maret, G., Wolf, P. E. Multiple Light Scattering from Disordered Media. The Effect of Brownian Motion of Scatterers. *Z. Phys. B - Condensed Matter*. **65**, 409–413 (1987).
34. Yu, G.Q. Near-infrared diffuse correlation spectroscopy in cancer diagnosis and therapy

monitoring. *Journal of Biomedical Optics*. **17** (1), (2012).
35. Carp, S. A., Dai, G. P., Boas, D. A., Franceschini, M. A., Kim, Y. R. Validation of diffuse correlation spectroscopy measurements of rodent cerebral blood flow with simultaneous arterial spin labeling MRI; towards MRI-optical continuous cerebral metabolic monitoring. *Biomedical Optics Express*. **1** (2), 553–565 (2010).
36. Roche-Labarbe, N. et al. Near-infrared spectroscopy assessment of cerebral oxygen metabolism in the developing premature brain. *Journal of Cerebral Blood Flow and Metabolism*. doi: 10.1038/jcbfm.2011.145 (2012).
37. Bergonzi, K. M., Bauer, A. Q., Wright, P. W., Culver, J. P. Mapping functional connectivity using cerebral blood flow in the mouse brain. *J Cereb Blood Flow Metab*. **35** (3), 367–370 (2015).
38. Poon, C. S., Li, J., Kress, J., Rohrbach, D .J., Sunar, U. Resting state Functional Connectivity measured by Diffuse Correlation Spectroscopy. *Optics InfoBase Conference Papers*. doi: 10.1364/TRANSLATIONAL.2018.JTh3A.63 (2018).
39. Li, J., Poon, C. -S., Kress, J., Rohrbach, D. J., Sunar, U. Resting state functional connectivity measured by diffuse correlation spectroscopy. *Journal of Biophotonics*. **11** (2), (2018).
40. Yu, G.Q. Near-infrared diffuse correlation spectroscopy in cancer diagnosis and therapy monitoring. *J Biomed Opt*. **17** (1), (2012).
41. Li, J. et al. Measurements of human motor and visual activities with diffusing-wave spectroscopy. *Novel Optical Instrumentation for Biomedical Applications II*. **5864**, 58640J, (2005).
42. Wang, D. et al. Fast blood flow monitoring in deep tissues with real-time software correlators. *Biomedical Optics Express*. **7** (3), 776 (2016).
43. Boas, D. A., Yodh, A. G. Spatially varying dynamical properties of turbid media probed with diffusing temporal light correlation. *Journal of the Optical Society of America a-Optics Image Science and Vision*. **14** (1), 192–215 (1997).
44. Diop, M., Lee, T.-Y., St. Lawrence, K. Continuous monitoring of absolute cerebral blood flow by combining diffuse correlation spectroscopy and time-resolved near-infrared technology. *Spie*. **7896**, 78960F, (2011).
45. Medical, I. *ISS Oxiplex Manual*. (2008).
46. Fantini, S. et al. Quantitative optical monitoring of the hemoglobin concentration and saturation in the piglet brain. doi: 10.1364/bosd.2000.wa3 (2014).
47. Hueber, D. M. et al. Non-invasive and quantitative near-infrared haemoglobin spectrometry in the piglet brain during hypoxic stress, using a frequency-domain multidistance instrument. *Physics in Medicine and Biology*. doi: 10.1088/0031-9155/46/1/304 (2001).
48. Zhang, J. et al. Application of I&Q detection system in scouting the curative effect of neck squamous cell carcinoma. *Optical Tomography and Spectroscopy of Tissue V*. doi: 10.1117/12.478177 (2003).
49. Zhao, J., Ding, H. S., Hou, X. L., Zhou, C. Le, Chance, B. In vivo determination of the optical properties of infant brain using frequency-domain near-infrared spectroscopy. *Journal of Biomedical Optics*. doi: 10.1117/1.1891345 (2005).
50. Tu, T., Chen, Y., Zhang, J., Intes, X., Chance, B. Analysis on performance and optimization of frequency-domain near-infrared instruments. *Journal of Biomedical Optics*. doi:

10.1117/1.1501562 (2002).
51. Choe, R. et al. Transabdominal near infrared oximetry of hypoxic stress in fetal sheep brain in utero. *Proceedings of the National Academy of Sciences of the United States of America*. doi: 10.1073/pnas.1735462100 (2003).
52. Sunar, U. et al. Noninvasive diffuse optical measurement of blood flow and blood oxygenation for monitoring radiation therapy in patients with head and neck tumors: a pilot study. *Journal of Biomedical Optics*. **11** (6), (2006).
53. Sunar, U. et al. Hemodynamic responses to antivascular therapy and ionizing radiation assessed by diffuse optical spectroscopies. *Optics Express*. doi: 10.1364/oe.15.015507 (2007).
54. Durduran, T., Choe, R., Baker, W. B., Yodh, A. G. Diffuse Optics for Tissue Monitoring and Tomography T. *Rep Prog Phys*. **73** (7), (2010).
55. Boas, D. A., Campbell, L. E., Yodh, A. G. Scattering and imaging with diffusing temporal field correlations. *Physical Review Letters*. doi: 10.1103/PhysRevLett.75.1855 (1995).
56. Boas, D. A., Yodh, A. G. Spatially varying dynamical properties of turbid media probed with diffusing temporal light correlation. *Journal of the Optical Society of America A*. doi: 10.1364/josaa.14.000192 (1997).
57. Chuang, C. -C., Sun, C. -W. Gender-related effects of prefrontal cortex connectivity: a resting state functional optical tomography study. *Biomedical Optics Express*. **5** (8), 2503 (2014).
58. Okamoto, M. et al. Multimodal assessment of cortical activation during apple peeling by NIRS and fMRI. *NeuroImage*. doi: 10.1016/j.neuroimage.2003.12.003 (2004).
59. Koessler, L. et al. Automated cortical projection of EEG sensors: Anatomical correlation via the international 10-10 system. *NeuroImage*. doi: 10.1016/j.neuroimage.2009.02.006 (2009).
60. Farzam, P. et al. Shedding light on the neonatal brain: Probing cerebral hemodynamics by diffuse optical spectroscopic methods. *Scientific Reports*. doi: 10.1038/s41598-017-15995-1 (2017).
61. Shang, Y., Li, T., Yu, G. Clinical applications of near-infrared diffuse correlation spectroscopy and tomography for tissue blood flow monitoring and imaging. *Physiological Measurement*. doi: 10.1088/1361-6579/aa60b7 (2017).
62. Mesquita, R. C. et al. Direct measurement of tissue blood flow and metabolism with diffuse optics. *Philos Trans A Math Phys Eng Sci*. **369** (1955), 4390–4406 (2011).
63. Durduran, T. et al. Diffuse optical measurement of blood flow, blood oxygenation, and metabolism in a human brain during sensorimotor cortex activation. *Optics Letters*. doi: 10.1364/ol.29.001766 (2004).
64. Kim, M. N. et al. Noninvasive measurement of cerebral blood flow and blood oxygenation using near-infrared and diffuse correlation spectroscopies in critically brain-injured adults. *Neurocritical Care*. doi: 10.1007/s12028-009-9305-x (2010).
65. Irwin, D. et al. Influences of tissue absorption and scattering on diffuse correlation spectroscopy blood flow measurements. *Biomedical Optics Express*. doi: 10.1364/boe.2.001969 (2011).

Figure 1

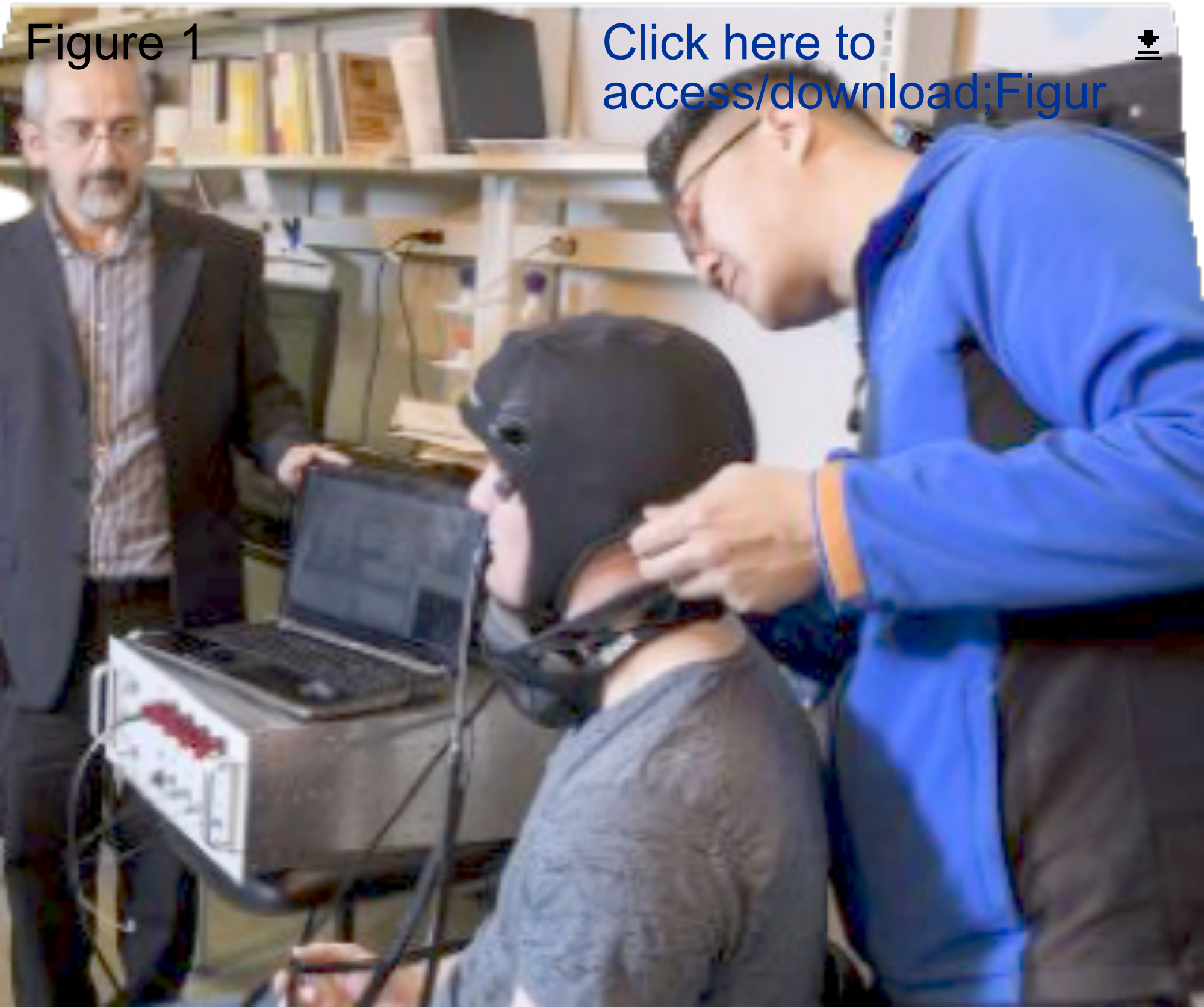

Figure 2

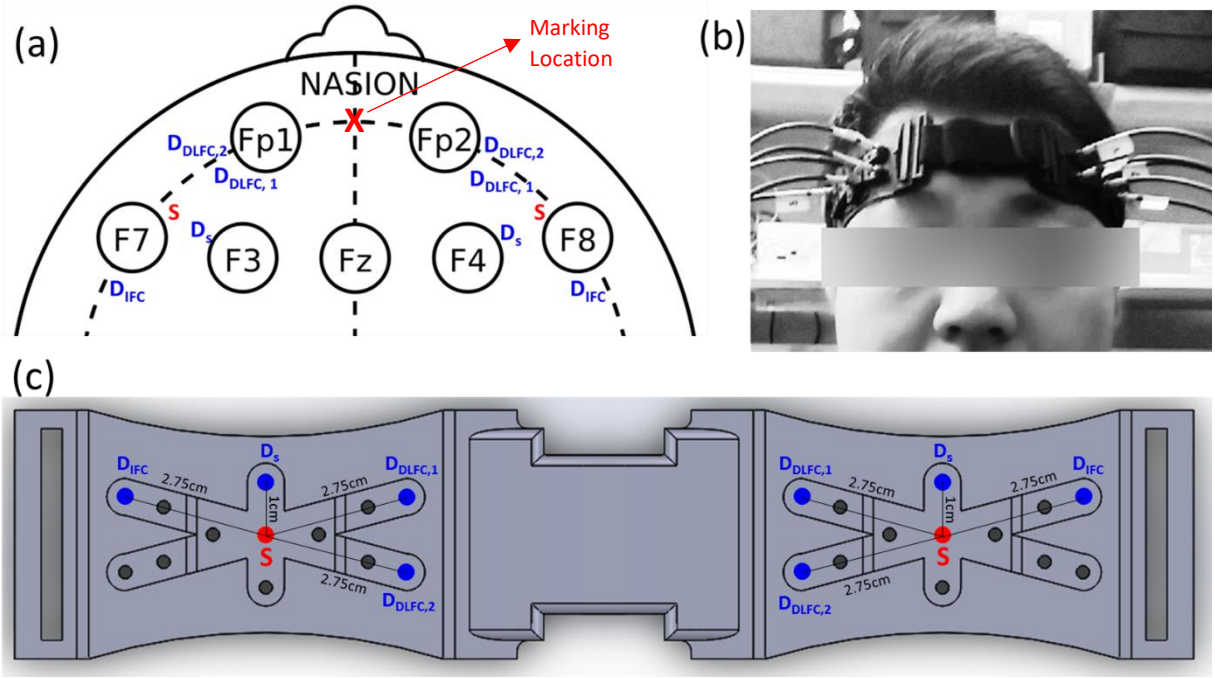

Figure 3

Click here to access/download;Figure;Fig3.pdf

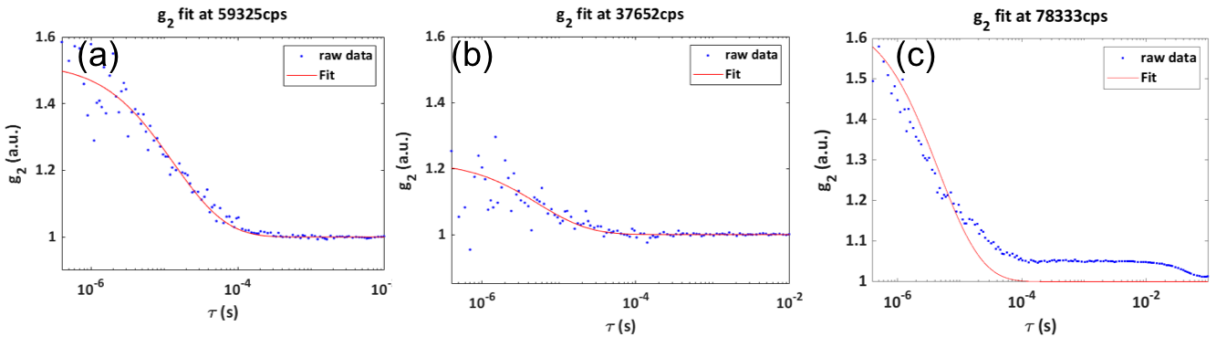

Figure 4

Click here to access/download;Figure;Fig4.pdf

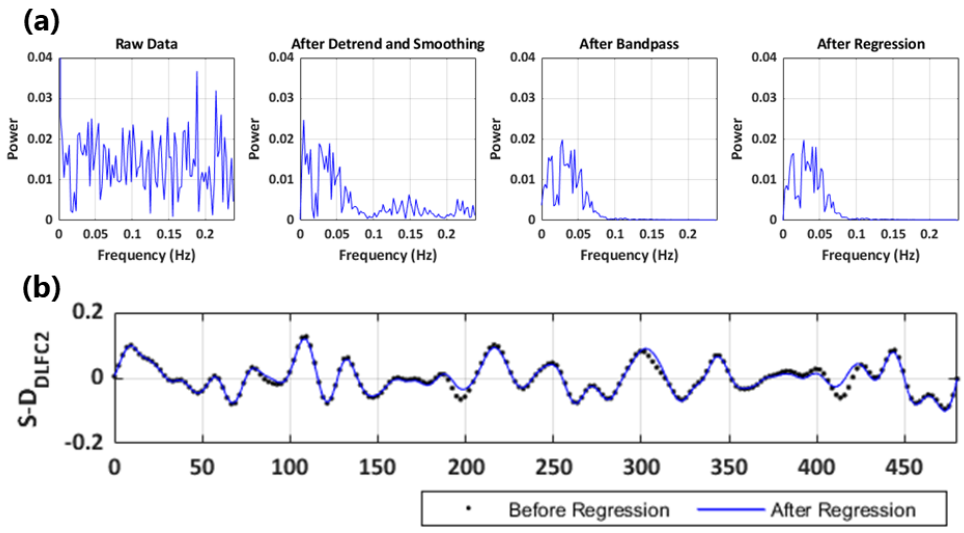

Figure 5

Click here to access/download;Figure;Fig5.pdf

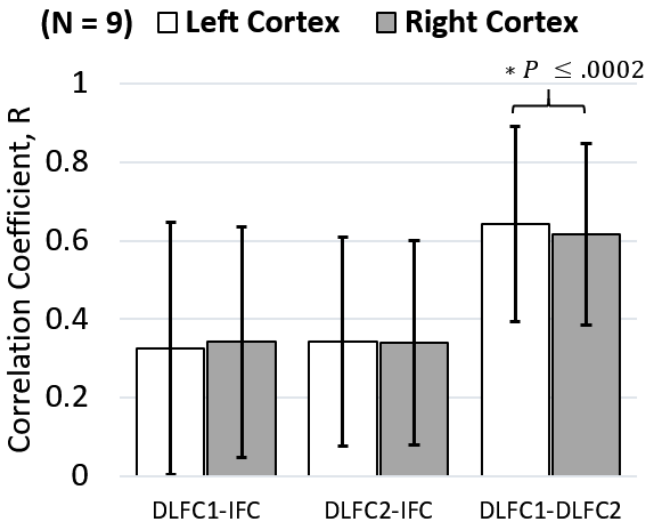

Table of Materials

Click here to access/download;Table of Materials;JoVE_Table_of_Materials_R2_Chien.xlsx

Name of Material/Equipment	Company	Catalog Number
3D Printed Probe	In-house	N/A
785nm, 100mW, CW, FC coupled Laser	CrystaLaser	DL785-100-S
Auto-correlator	Correlator.com	Flex05-8ch
Data Acquisition GUI	In-house	N/A
Data analysis software	In-house	N/A
EEG Electrode Cap	OpenBCI	N/A
Multi-mode fiber	OZ Optics	QMMJ-3,2.5-IRVIS-600/630-3PCBK-3
Oxiplex calibration phantom	ISS	75019, 75020
Oxiplex muscle probe	ISS	86010
Oxiplex Oximeter	ISS	95205
Power meter	Thorlabs	PM100D
Sensor card	Thorlabs	F-IRC1-S
Single-mode fiber	OZ Optics	SMJ-3S2.5-780-5/125-3PCBK-3
Single-Photon Counting Machine	Excelitas	SPMC-NIR-1x2-FC

Comments/Description
3D printed PLA probe (Craftbot, Craft unique)
DCS component (light source)
DCS component (output g2 curve to PC)
GUI coded in LabVIEW to run the DCS system
Matlab code used for obtaining RSFC results
EEG mesh cap with standard 10/20 positions
DCS component (source fiber)
Set of 2 PDMS Calibration Phantom
4 channel muscle probe
FD-fNIRS (690nm, 830nm)
Laser light power adjuster
laser IR beam viewer
DCS component (detector fiber)
DCS component (detector)

We thank the reviewers for their time and efforts. We have carefully considered the points raised by the reviewers and revised the manuscript accordingly. Our responses to specific reviewer comments are given below.

Reviewer #1:

General Questions :

What is the motivation behind this work? Why did the authors use DCS instead of using fNIRS? What is the contribution of this choice to the literature?

Here the motivation is to show that optical CBF can be used to assess RSFC in humans, DCS can be used in addition to fNIRS approach. The contribution is additional CBF parameter for RSFC analysis in human applications.

Minor concerns:

* Line 41: Inter-regional RSFC is significantly stronger than inter-regional RSFC ? I think the first "inter" should be "intra".

Thank you for the correction, yes, we have revised that sentence accordingly.

" correlation in intra-regional RSFC is significantly stronger than the inter-regional RSFC"

* Line 51: "Abnormalities in RSFC have been associated with neuronal disorders such as autism, Alzheimer's, and depression." Please cite the related studies in this sentences as "such as autism (author (s), year), Alzheimer's (author(s), year), depression (author(s), year).

Agreed, we have cited these accordingly.

> *Li, J., Qiu, L., Xu, L., Pedapati, E. V., Erickson, C. A., & Sunar, U. (2016). Characterization of autism spectrum disorder with spontaneous hemodynamic activity. Biomedical optics express, 7(10), 3871-3881. This is for autism*
>
> *Sheline, Y. I., & Raichle, M. E. (2013). Resting state functional connectivity in preclinical Alzheimer's disease. Biological psychiatry, 74(5), 340-347. For Alzheimer's*
>
> *Mulders, P. C., van Eijndhoven, P. F., Schene, A. H., Beckmann, C. F., & Tendolkar, I. (2015). Resting-state functional connectivity in major depressive disorder: a review. Neuroscience & Biobehavioral Reviews, 56, 330-344. For depression*

* Line 53-55: "However, many such patients, such as young autistic children, are poor candidates for assessment by fMRI, which requires patients to hold still for long intervals inside a confined imaging

space with loud noise from the magnet." Is there an evidence in literature about this? If there is, please cite.

We cited 2 sample publications, and removed “with loud noise from the magnet”:

> *Kiviniemi, V., Jauhiainen, J., Tervonen, O., Pääkkö, E., Oikarinen, J., Vainionpää, V., ... & Biswal, B. (2000). Slow vasomotor fluctuation in fMRI of anesthetized child brain. Magnetic Resonance in Medicine: An Official Journal of the International Society for Magnetic Resonance in Medicine, 44(3), 373-378.*
>
> *In this article children were anesthetized to secure a motionless state.*
>
> *Fransson, P., Skiöld, B., Horsch, S., Nordell, A., Blennow, M., Lagercrantz, H., & Åden, U. (2007). Resting-state networks in the infant brain. Proceedings of the National Academy of Sciences, 104(39), 15531-15536.*
>
> *In this article, infants were given a low dose of the sedative agent chloral hydrate (30 mg/kg orally or rectally) with sustained spontaneous breathing, were anesthetized to secure a motionless state.*

* Line 78-79 : "have been successfully used for functional brain imaging in pediatric and even in very young infants" Please add some studies about pediatry and very young infants.

We have added representative citations accordingly.

> *Durduran, Turgut, and Arjun G. Yodh. "Diffuse correlation spectroscopy for non-invasive, micro-vascular cerebral blood flow measurement." Neuroimage 85 (2014): 51-63.*
>
> *Buckley, E. M., Parthasarathy, A. B., Grant, P. E., Yodh, A. G. & Franceschini, M. A. Diffuse correlation spectroscopy for measurement of cerebral blood flow: future prospects. Neurophotonics (2014). doi:10.1117/1.nph.1.1.011009*
>
> *D.R., B. et al. Cerebral blood flow response to hypercapnia in children with obstructive sleep apnea syndrome. Sleep (2015).*
>
> *Buckley, E. M. et al. Cerebral hemodynamics in preterm infants during positional intervention measured with diffuse correlation spectroscopy and transcranial Doppler ultrasound. Opt. Express (2009). doi:10.1364/oe.17.0125711.*
>
> *Durduran, T. et al. Optical measurement of cerebral hemodynamics and oxygen metabolism in neonates with congenital heart defects. J. Biomed. Opt. (2010). doi:10.1117/1.3425884*
>
> *T., D. et al. Cerebral oxygen metabolism (CMRO2) reactivity to hypercapnia in neonates with severe congenital heart defects measured with diffuse optics. J. Cereb. Blood Flow Metab. (2009).*
>
> *Dehaes, M. et al. Cerebral oxygen metabolism in neonatal hypoxic ischemic encephalopathy during and after therapeutic hypothermia. J. Cereb. Blood Flow Metab. (2014). doi:10.1038/jcbfm.2013.165*

Lin, P. Y. et al. Non-invasive optical measurement of cerebral metabolism and hemodynamics in infants. J. Vis. Exp. (2013).

Lin, P. Y. et al. Regional and hemispheric asymmetries of cerebral hemodynamic and oxygen metabolism in newborns. Cereb. Cortex (2013). doi:10.1093/cercor/bhs023

* Section 1.5 : Instead of using the term "inter or intra-brain" please use "inter or intra-hemispheric". Because the term "inter-brain" is used for multi subject based studies such as social interaction, hyperscanning etc.

Thank you for the comment. We have changed the use of terms accordingly.
"this would be the boundaries between the superior prefrontal cortex and the dorsolateral prefrontal cortex (DLFC), and between DLFC and the inferior prefrontal cortex (IFC), respectively, for the left and right hemisphere."

How did you decide these regions? Inter-subject variability and cortical morphology might be different. Please utilize the fNIRS studies, Okamoto et al., 2004 and Koessler et al., 2009.

We have chosen the left and right dorsolateral frontal cortex (DLFC) as the intra-regional connectivity as it is typically shown to be stronger as compared to inter-regional connectivity between the inferior frontal cortex (IFC) and the DLFC. Inter-subject variability exists, and it is the cause of the large error bars on Fig 5. However, the general trend that intra-regional connectivity is stronger than inter-regional connectivity still holds. We have used the EEG 10-20 system carefully as best as we can to attempt in minimizing errors arising from cortical morphology differences.

* Section 5.2. What is the threshold for g2(tau) for analysis? Did you use a fixed Beta?

Threshold for g2(tau) is from 0.4us to 0.1s. Beta was fitted.

* Section 5.5 How did you decide this pass-band frequency? Did you decide the frequency by considering only filtering purposes? or is there any previous fMRI, fNIRS or ASL study that provided evidence before about this frequency band?

We have used a band-pass filter with the pass band of [0.009 0.08 Hz], because this band has been used in several fNIRS studies for accessing resting-state functional connectivity. We have added these representative references.

B. R. White, A. Z. Snyder, A. L. Cohen, S. E. Petersen, M. E. Raichle, B. L. Schlaggar, and J. P. Culver,"Resting-state functional connectivity in the human brain revealed with diffuse optical tomography," Neuroimage 47(1), 148–156 (2009).

R. C. Mesquita, M. A. Franceschini, and D. A. Boas, "Resting state functional connectivity of the whole head with near-infrared spectroscopy," Biomed. Opt. Express 1(1), 324–336 (2010).

* Please provide some time series for general assessment. Especially, before and after band-pass filtering and short channel regression.

We have added a new figure (Fig 4) to show an example of the time series and the power spectrum at each processing step.

* Line 212 : What is 23, 24 and 34? How do they represent the regions? Please provide a more clear explanation. If I understand correctly, 23 represents the correlation between detector number 2-3 and the rest is the same. If this is the method to define, 2 seems a short distance channel, compared with other channels and used for measuring the scalp.

Detector 2 is located in the IFC, detector 3 & 4 are located in the DLFC, detector 1 (not shown) is the short distance. The text revised to clarify these.

* Line 252 : "To determine whether CBF measured by DCS could accurately detect RSFC" RSFC is a whole brain-based approach which includes several brain regions that some of them cannot be measured by using optical techniques. This statement is assertive and should be modified.

The reviewer brings up a very valid point for brain imaging and agreed. This sentence is modified as "To determine whether CBF measured by DCS could accurately detect RSFC for the superficial cortical regions in prefrontal locations"

* Line 255 - 256: Please provide some evidence about "strong intra-regional connectivity" and "weaker inter-regional connectivity" in resting state functional connectivity.

RSFC reflects the synchronicity of spontaneous activity in functionally related regions in the brain, which may imply the connectivity is higher within a functional region, while weaker between different functional regions.

Reviewer #2:

Line 102,step 1.6: please provide more detail about creation of the 3D-printed probe

3D printed probe is designed with Solidworks and printed with a commercially available 3D printer (Craftbot, CraftUnique) and flexible TPU filament (Ninjaflex). The text is revised to add this detail.

Line 195, step 5.7: what type of correction for multiple comparisons is recommended for this type of correlation analysis? (this is mentioned later on line 211 but should be mentioned in step 5.7 as a standard procedure)

We have added more details to step 5.6-5.8 accordingly.

"5.6) Use linear regression to obtain the residuals from each channel against the short distance measurement to remove the superficial scalp signals on each side of the cortex (Fig. 4b).
5.7) Calculate the Pearson's correlation coefficient between each pair of channels to identify the resting state functional connectivity between brain regions (Fig. 5).
5.8) Transform the correlation value into z-value using fisher's Z transform and perform a t-test to obtain the P value (Fig. 5).False discovery rate (FDR) was used for multiple comparisons correction.

Please provide more details about the spatial and temporal resolution of these measurements

This is a spectroscopic point measurement with a max SD of 2.75cm, with a spatial resolution of ~2.75 cm. Temporal resolution was ~2s due to signal averaging.

The authors state that there are established patterns of functional connectivity between DLFC regions and between DLFC and IFC in the discussion, but citations are lacking to back up this key point.

We have revised that sentence and added a representative citation accordingly.

> *Chuang, Ching-Cheng, and Chia-Wei Sun. "Gender-related effects of prefrontal cortex connectivity: a resting-state functional optical tomography study." Biomedical optics express 5.8 (2014): 2503-2516.*

Lines 259-263. The last 3 sentences of the discussion are overstated and not appropriately worded. The results presented here may be encouraging and may suggest that DCS can map functional connectivity in the human brain, but these preliminary results in 9 subjects do not "prove the potential" of DCS for this purpose. Similarly, the next sentence overstates the translational impact of this technique, because it is not evidence that the technique is ready to provide "accurate characterization of neuronal diseases." I would recommend wording these sentences more cautiously and conservatively.

Agreed, and we thank the reviewer for the suggested wording. We have revised the discussion accordingly.

Line 268-272: "These results suggest that DCS can assess RSFC in humans for improved characterization of the human brain function. This approach can easily complement other techniques such as fNIRS to become a highly useful tool for non-invasive assessment of brain function in young and disabled patients."

It would be helpful if the abstract provided at least one sentence summarizing the results of the 9-subject analysis.

Agreed, thank you for the suggestion. We have added a sentence summarizing the results.

"has shown that the intra-regional RSFC is significantly higher (0.64 ± 0.25) on the left cortex and (0.62 ± 0.23) on the right cortex as compared to the inter- regional RSFC (0.32 ± 0.32), (0.34 ± 0.27) on the left cortex and (0.34 ± 0.29), (0.34 ± 0.26) on the right cortex."

There are many grammatical errors in this manuscript that need to be corrected. For example,

line 38: "DCS provides a key hemodynamics variable" should be "DCS provides a key hemodynamic variable"

Thank you for the comment. We have corrected that sentence.

"DCS provides a key hemodynamic parameter"

line 41: Some sentences do not make sense:

"Therefore, DCS is used to measure CBF-based RSFC in human frontal cortex and found the inter-regional RSFC is significantly stronger than the inter-regional RSFC". Presumably, the authors meant to say "intra-regional".

Thank you for the comment. We have corrected that sentence accordingly.

" correlation in intra-regional RSFC is significantly higher than the inter-regional RSFC"

Line 50: why are two optical references (9 and 10) used in a sentence about resting-state fMRI?

There seems like reference editor mixed up between endnote and Mendeley. Ref 9 and 10 are removed.

Line 51-52: please provide citations

Thank you for the suggestion. We have cited these accordingly.

> *Li, J., Qiu, L., Xu, L., Pedapati, E. V., Erickson, C. A., & Sunar, U. (2016). Characterization of autism spectrum disorder with spontaneous hemodynamic activity. Biomedical optics express, 7(10), 3871-3881. This is for autism*
>
> *Sheline, Y. I., & Raichle, M. E. (2013). Resting state functional connectivity in preclinical Alzheimer's disease. Biological psychiatry, 74(5), 340-347. For Alzheimer's*
>
> *Mulders, P. C., van Eijndhoven, P. F., Schene, A. H., Beckmann, C. F., & Tendolkar, I. (2015). Resting-state functional connectivity in major depressive disorder: a review. Neuroscience & Biobehavioral Reviews, 56, 330-344. For depression*

Line 100: please define all acronyms at first use (DLFC and IFC)

Thank you for the suggestion. We have defined those terms at first use.

"between dorsolateral prefrontal cortex (DLFC) and the inferior prefrontal cortex (IFC) of"

Reviewer #3:

The analysis doesn't seem too strong regarding - statistical rigourness and reasoning behind using both parametric and non-parametric approaches, and correcting for multiple comparisons. Authors show the P-values with error bar in Fig.5. but it is not clear the error bar means. Just based on the plot it might be standard deviation and thus further comparison of the P-values came out to be statistically significant (Fig.6.) Otherwise it doesn't seem convincing that the correlation in site 23 and 34 are statistically different as the Authors claim.

We have consolidated figure 5 and 6 and have reported the P-values to provide statistical rigor. Specifically, we have performed the correlation coefficient, R, and have transformed it into a Z value with the Fisher's Z transform. Lastly the P value is obtained by using a T-test.

Authors should discuss why used Pearson and Fisher's z transform to begin with: These are parametric approaches that requires normality but it is not very clear the assumption was met. Otherwise Spearman correlation should be considered. Likewise, non-parametric test (Rank sum) was used for comparing INTRA and INTER connectivity without explaining the reader why.

We agree with the reviewer. The Fisher's z transform was applied to the correlation coefficient, which makes the data more Gaussian, thus the t-test can be performed. We provided t-test results in the revised text. The analysis showed that the intra-regional RSFC in DLPFC is significantly stronger than the intra-regional RSFC (between DLFC and IFC).

Finally, it is not clear that the final P-values = 0.004 (Fig.6.) was observed after correcting/penalizing for multiple comparisons. In this work there is at least two comparisons DLFC-to-DLFC sites and DLPFC-to-IFC sites. If these concerns can be solved then the work presented here can be more solid.

Agreed. In the revised version, Fig.6 is deleted. For the multiple comparisons we used false discovery rate (FDR) correction.

Minor Concerns:

Typos- Line41 "inter-regional" appeared twice.. I think the authors meant "the intra-regional RSFC is stronger than the inter-regional RSFC"

Thank you for the comment. We have corrected the above comments accordingly.

" correlation in intra-regional RSFC is significantly stronger than the inter-regional RSFC"

Can mislead - Line 69: DCS does not quantify "absolute" CBF. CBFi is still a relative measure, even though authors described as "absolute ... related contrast" because it is difficult to know the "contrast" (I understood the "contrast" as an absolute reference point) in such non-invasive measurements.

We agree. We have corrected the above comments accordingly.

"cells which can quantify cerebral blood flow – a key hemodynamic parameter."

Clarity - Line96-101: Authors could revise the writing such that how/where the marking done is clearly visible as well in Fig.2a. There are terms that were not defined in the earlier text (DLFC and IFC, but defined later in Discussion)

Thank you for the comment. We have corrected the above comments accordingly.

"1.3) Mark the location with a marker at the first 10% of the distance between the two points (nasion to the inion) to locate the point between Fp1 and Fp2 of the EEG 10/20 montage (Fig. 2a).

1.4) Using an EEG 10/20 cap, adjust the cap so that the marked point is between Fp1 and Fp2.

1.5) Mark the point between Fp1 and F7 (left cortex) and the point between Fp2 and F8 (right cortex). This would be the boundaries between the superior prefrontal cortex and the dorsolateral prefrontal cortex (DLFC), and between DLFC and the inferior prefrontal cortex (IFC), respectively, for the left and right hemisphere. Fig. 2a).

Clarity - Line 157 and 188: Please explain how LONG is long about g2 curves should go to 1 for "LONG correlation time" or "LARGER times". For example, 10^-2sec?

Thank you for the comment. We have corrected the above comments accordingly.

"autocorrelation curve decays to 1 for longer correlation time (>10ms)"

"(2) if the autocorrelation curve does not decay to 1 for longer correlation time (>10ms), like"

Clarity - Line 187 0.5--> 1.5? 0.2 --> 1.2? You could stay in the beta scale of 1~.

Thank you for the comment. We have made the sentence clearer.

"autocorrelation function is significantly lower than 1.5 ($\beta < 0.5$), for example like in the case of Fig. 3b where the function is ~1.2 ($\beta < 0.2$)due to room light leakage."

Clarity - Line 189 What type of motion artifacts? Will simple head move can disrupt g2 so much? Some description will be helpful.

"where the motion artifact (e.g. jerking, head movement, probe fiber movement) lead to this type of data"

Typo?/Clarity - Fig.6: Why is the LEFT PFC showed significant INTER-INTRA brain contrast in CASE:24-34, but not on the RIGHT side? On the RIGHT side the 23-34 group showed difference. This plot may be replace by a table. Again, how was the multiple comparisons problem being addressed when reporting the P-values?

Both left and right p values are below 0.05, so all of them are significant. We have consolidated this figure to fig 5 and have reported the P-values to provide statistical rigor.

Reviewer #4:

Whole procedure is written, not like a scientific paper, but like a technical manual. The writing style has to change so that each sentence is complete, and only informative and relevant contents should be written. Sentences like 'Do not look at the light source' are totally inappropriate for a scientific paper, and it almost feels like the authors have copied a section of a manual into this manuscript.

This journal format is slightly different than other journals. We have selected this writing style to suit JOVE, which focused on the experimental protocol.

The optode positions appearing in Fig 2 (c) and (d) do not match each other, and it is difficult to understand what region of the brain the optodes are probing, as there is no depiction of human brain in the figure.

The optode numbers refers to the channel ID used in the DCS instrument and is only for illustration purposes. They are removed to prevent confusion.

Also, what would be the reason behind selecting DLPR and IPF, other than the fact that it is easy to place optodes on the forehead?

We have chosen the left and right dorsolateral frontal cortex (DLFC) as the intra-regional connectivity as it is typically shown to be stronger as compared to inter-regional connectivity between the inferior frontal cortex (IFC) and the DLFC.

It is not very clear how the optical properties measured by FD-NIRS are used in calculation or calibration of DCS reading. Also, the fundamental limitation in the protocol is that FD-NIRS and DCS are done sequentially, not concurrently. Any plan or strategy to get around this issue?

Optical properties were measured by amplitude decay and phase fit with a multi-distance method with ISS provided self calibrated phantoms and probes on the forehead. We used this value fixed for each subject at each RSFC point.

The reviewer raises a valid point indicating experimental limitation of this approach (which are added in our Discussion section as the limitations) in that the main challenge in the field is concurrent measurements of NIRS/DCS to provide optical parameters as input for DCS. Several approaches have been done, as called hybrid instruments with time sharing by sequentially turning on the NIRS and DCS light sources. One can turn on the NIRS light source, perform the acquisition, and then turn it off, and then turn on the DCS light source. In our pilot study, we chose the isolated, lighter DCS probe with a better contact. In the future, the probe design can be improved, then NIRS fibers can be inserted next to DCS fibers, and light sources can be sequentially illuminated as previously demonstrated[refs].

Durduran, T. & Yodh, A. G. Diffuse correlation spectroscopy for non-invasive, micro-vascular cerebral blood flow measurement. NeuroImage (2014).doi:10.1016/j.neuroimage.2013.06.017

Farzam, P., Buckley, E. M., et al. Shedding light on the neonatal brain: Probing cerebral hemodynamics by diffuse optical spectroscopic methods. Scientific Reports (2017).doi:10.1038/s41598-017-15995-1

Shang, Y., Li, T. & Yu, G. Clinical applications of near-infrared diffuse correlation spectroscopy and tomography for tissue blood flow monitoring and imaging. Physiological Measurement (2017).doi:10.1088/1361-6579/aa60b7

Mesquita, R. C. et al. Direct measurement of tissue blood flow and metabolism with diffuse optics. Philos. Trans. R. Soc. A Math. Phys. Eng. Sci. (2011). doi:10.1098/rsta.2011.0232

Durduran, T. et al. Diffuse optical measurement of blood flow, blood oxygenation, and metabolism in a human brain during sensorimotor cortex activation. Opt. Lett. (2004). doi:10.1364/ol.29.001766

Yu, G. Diffuse Correlation Spectroscopy (DCS): A Diagnostic Tool for Assessing Tissue Blood Flow in Vascular-Related Diseases and Therapies. Curr. Med. Imaging Rev. (2012). doi:10.2174/157340512803759875

Kim, M. N. et al. Noninvasive measurement of cerebral blood flow and blood oxygenation using near-infrared and diffuse correlation spectroscopies in critically brain-injured adults. Neurocrit. Care (2010). doi:10.1007/s12028-009-9305-x

Irwin, D. et al. Influences of tissue absorption and scattering on diffuse correlation spectroscopy blood flow measurements. Biomed. Opt. Express (2011). doi:10.1364/boe.2.001969

T., D. et al. Cerebral oxygen metabolism (CMRO2) reactivity to hypercapnia in neonates with severe congenital heart defects measured with diffuse optics. J. Cereb. Blood Flow Metab. (2009).

Dehaes, M. et al. Cerebral oxygen metabolism in neonatal hypoxic ischemic encephalopathy during and after therapeutic hypothermia. J. Cereb. Blood Flow Metab. (2014). doi:10.1038/jcbfm.2013.165

Lin, P. Y. et al. Non-invasive optical measurement of cerebral metabolism and hemodynamics in infants. J. Vis. Exp. (2013).

Lin, P. Y. et al. Regional and hemispheric asymmetries of cerebral hemodynamic and oxygen metabolism in newborns. Cereb. Cortex (2013). doi:10.1093/cercor/bhs023

Also, the theoretical part has to be strengthened so that readers can understand what DCS exactly measures. In fact, this is the first time the reviewer has seen a DCS paper without even an equation or variable definition.

For JOVE format we did not want to add theoretical part, in the revised form we have added some details.

Did authors use Brownian motion model to fit the decaying autocorrelation curve? On what basis? Does high DCS measurement correspond to faster blood cell motion or larger flow volume, or both?

Both. We used the Brownian motion model as it has been demonstrated to represent sufficiently accurate model for the data in humans and animals [see recent review by Durduran/Yodh 2014]. Here, decay rate represents blood cell speed and blood volume fraction.

-Abstract 2nd line : key hemodynamic variable

-Abstract 6th line : critical typo exists, where inter and intra are used wrongly.

Thank you for the comment. We have corrected the above comments accordingly.

" correlation in intra-regional RSFC is significantly stronger than the inter-regional RSFC"

"cells which can quantify cerebral blood flow – a key hemodynamic parameter."

-Introduction, 2nd paragraph : Specify what cross-correlation frequency means.

Thank you for the question. Here the cross-correlation frequency represents the lower frequency that is produced after heterodyning. It is typical of frequency domain systems.

-Introduction 3rd paragraph : It is not exactly right to explain that the measured intensity fluctuates faster for faster moving blood cells, as the decay rate of autocorrelation curve depends not on the fluctuating frequency, but on how fast the signal looses its self-similarity.

Thank you for the comment. We have corrected those sentences accordingly.

"in time which produces the intensity autocorrelation function. With faster moving blood cells, the autocorrelation function decays faster due to the decrease of correlation in time. "

-Protocol 1.5 : … point that is between …

-Protocol 1.6 : … on both the …

Thank you for the comment. We have corrected those sentences accordingly.

“Mark the point between Fp1 and F7 (left cortex) and the point between Fp2 and F8”

“Using a 3D printed probe; place the multi-mode fibers on the newly marked points and”